Cosmic-ray and SEP physics with the LISA missions

Catia Grimani
Istituto di Fisica
Università di Urbino Carlo Bo
Urbino, Italy
Email: cgrimani@fis.uniurb.it

Michele Fabi
Istituto di Fisica
Università di Urbino Carlo Bo
Urbino, Italy
Email: m.fabi@fedux.uniurb.it

***Abstract*— The LISA (Laser Interferometer Space Antenna) and LISA Pathfinder (LISA-PF) spacecraft will be equipped with particle detectors to monitor p and He nucleus fluxes above a few tens of MeV(/n) at all times. Both missions are expected to take data during different solar modulation and, possibly, different polarity periods. We will be able to monitor both variations and fluctuations of galactic cosmic-ray (GCR) fluxes as well as solar energetic particle (SEP) transit. The LISA mission in particular, will allow us to map SEPs over 2° in longitude at once. Particle observations on board the LISA missions are of great interest to cosmic-ray, solar physics and space weather investigations.**

I. Introduction

LISA is the first ESA/NASA mission dedicated to the detection of gravitational waves in space in the frequency range 10^{-4} - 0.1 Hz unseen by terrestrial detectors above gravity gradient noise of the Earth (http://lisa.jpl.nasa.gov). It consists of three spacecraft located at the corners of an equilateral triangle of 5×10^6 km side forming a Michelson interferometer. Each spacecraft hosts optical telescopes and two inertial sensors. The heart of the inertial sensors is a cubic Pt/Au test mass constituting the mirrors of the Michelson interferometer and defining the arm lengths. The test masses must remain, nominally, in pure geodesic motion. The spacecraft shield the test masses by external disturbances, such as solar radiation pressure. A set of electrodes forms a capacitive gravitational reference sensor for sensing and actuation of the test-mass position. The gravitational reference sensor measurements are used to control μN thrusters on the spacecraft to force it to follow the test masses (drag-free control). Forces acting directly on the test masses cannot be shielded. Galactic and solar nuclei with energies larger than 100 MeV(/n) and electrons above a few MeV deposit charge in the test masses [1]–[3]. Spurious forces occur between the test masses and the surrounding electrodes mimicking gravitational wave signals. A UV-light system will be located on board to discharge the test masses via the photoelectric effect [4], [5]. In order to control the test-mass charging, it has been found as necessary to place particle detectors in each spacecraft.

LISA is tentatively scheduled to be launched in 2015. The nominal mission lifetime is 2 years with a possibility to extend it up to 10 years. A technology mission for LISA, the LISA-PF, will be launched in 2009. LISA-PF is supposed to provide a testing ground to measure the level of charging disturbances and to test the charge management system for LISA. LISA-PF consists of one spacecraft hosting two 30 cm distant test masses. Expected mission duration is six months.

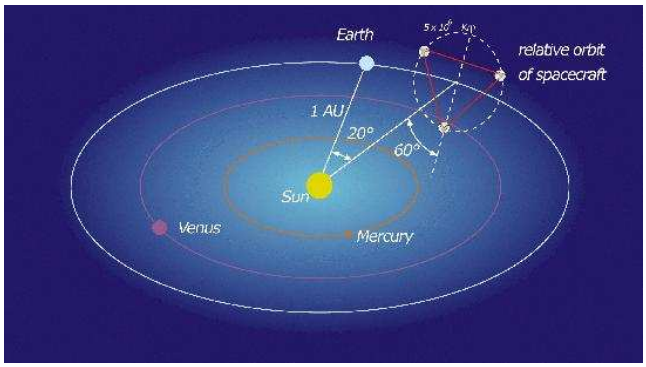

Fig. 1. LISA orbit.

The LISA-PF design of the particle monitors will allow us to detect galactic p and ^{4}He nucleus flux variations and fluctuations related to different solar modulation and polarity epochs and/or of interplanetary origin. No electron and heavy ion detection is permitted at this stage [6].

The simulation of the LISA test-mass charging due to the galactic cosmic-ray nuclei and interplanetary electrons during different solar polarity periods has shown that these *rare* particles account for 20% of the total test-mass charging [7]. Consequently, radiation monitors for electrons and heavy nuclei for the LISA mission are strongly recommended.

II. LISA and LISA-PF orbit characteristics

The LISA orbit with respect to Earth and Sun is sketched in Fig. 1. The center of the spacecraft formation is on the ecliptic plane, 20° behind the Earth. The three spacecraft rotate about the center of the formation in the plane of the triangle that is inclined at 60° with respect to the ecliptic plane. One rotation lasts one year. Spacecraft longitude covers a range of approximately 2° and their distance from the Sun varies between 149 and 152 $\times$ 10^6 km. Details are summarized in Table 1. In Fig. 2 we have reported the LISA-PF orbit. One spacecraft will be placed in orbit in L1 at 1.5 $\times$ 10^6 km from Earth.

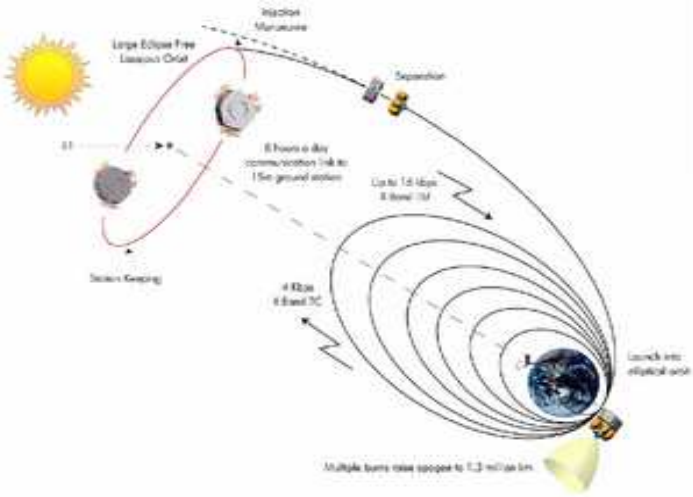

Fig. 2. LISA-PF orbit.

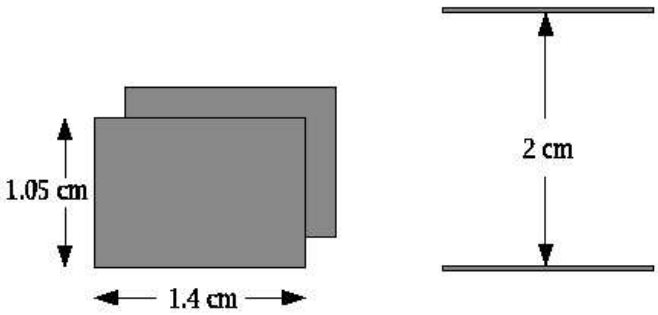

Fig. 3. Geometrical characteristics of the radiation monitors.

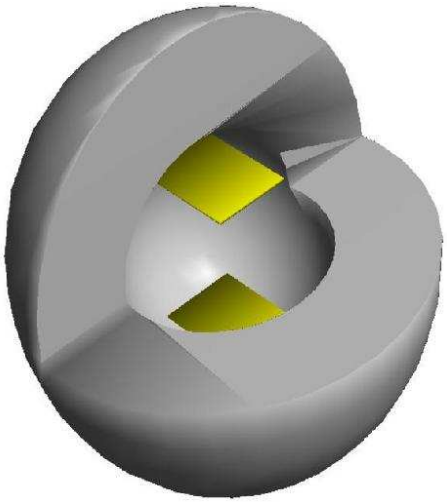

Fig. 4. Pictorial view of the radiation monitor set-up.

TABLE I
LISA SPACECRAFT ORBIT CHARACTERISTICS

Distance from the Sun	$149 \div 152 \times 10^6$km $0.9933 \div 1.0133$ AU
Latitude off the ecliptic	$0.7° \div 1.0°$
Longitude difference with respect to Earth	$19° \div 21°$

III. LISA-PF RADIATION MONITOR DESIGN

The charge deposited onto the test masses generates spurious forces that increase the acceleration noise limiting the sensitivity of the interferometer mainly at low frequencies. Particle monitors will provide a real time estimate of the incident flux of galactic and solar particles allowing the optimization of the test-mass discharging, the improvement of the duty cycle of the interferometer (on-line) and noise estimate (off-line).

Particle monitor present design consists of two silicon wafers of 1.4 x 1.05 cm^2 area, 300 μm thickness forming a small telescope (see Fig. 3 for details). Silicon telescopes are surrounded by a 1.32 cm titanium shell, corresponding to 6 g/cm^2 of matter (Fig. 4). The front-end electronics dynamic range is 50 keV - 5 MeV and therefore we will be able to discriminate protons and helium nuclei of galactic and solar origin but no ^{3}He - ^{4}He, electrons or heavy nucleus identification will be possible.
The geometrical factor for isotropic incidence on one silicon layer is 9.24 cm^2 sr while for both detectors (coincidence events) is 0.87 cm^2 sr.

IV. SOLAR MODULATION, SOLAR POLARITY AND NORTH-SOUTH ASYMMETRY

Long-term cosmic-ray variations are correlated with the 11-year solar cycle and the 22-year global solar magnetic field (GSMF) polarity period. In Fig. 5 we have reported the expected level of solar modulation and solar polarity epochs at the time of the two LISA missions.

During a solar cycle the observed sun-spot number rises from a low to a maximum value and then returns to a low value. Cosmic-ray intensity is observed to be inverse with respect to the solar activity. When the level of solar activity is high the solar wind is more effective in preventing galactic cosmic rays to enter the solar cavity, mainly at low energies. It is found that solar modulation is related to distance from the Sun and latitude. In [8] it is shown that cosmic-ray observations gathered near Earth can be used for LISA test-mass charging simulation at both solar minimum and maximum. The solar modulation effect on proton and helium fluxes measured near Earth is shown in Figs. 6 and 7.
The Sun has a complex magnetic field, however, the dipole term approximately always dominates the magnetic field in the solar wind. The projection of this dipole on the solar rotation axis (A) can be either positive, which we refer to A$>$0 state, or negative, wich we refer to A$<$0 state. At each

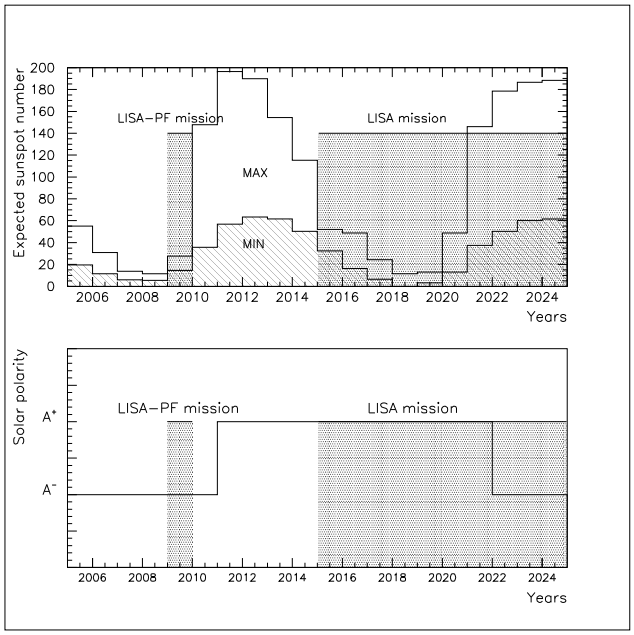

Fig. 5. Expected maximum (white area) and minimum (dashed area) solar activity level (top figure) and solar polarity epochs (bottom figure) at the time of the LISA missions.

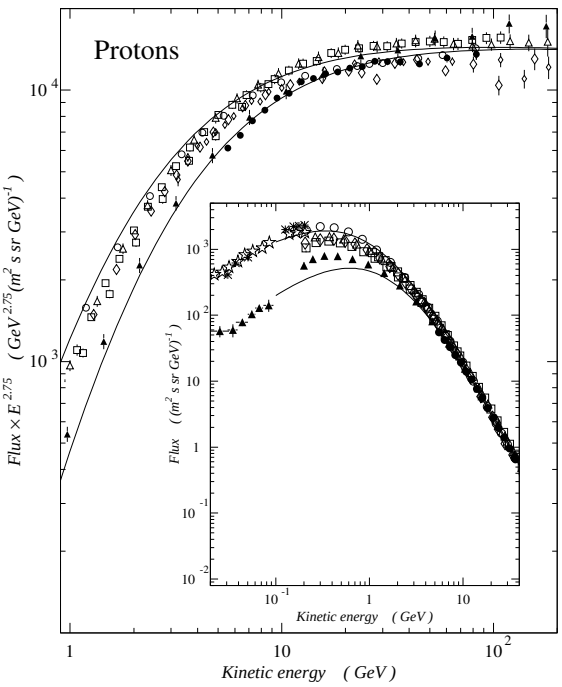

Fig. 6. Cosmic-ray proton measurements during various solar modulation periods. Curves represent the best fit to data at solar minimum (top curve) and solar maximum (bottom curve). References and details are reported in [8].

sunspot maximum, the dipole reverses direction, leading to alternating magnetic polarity in successive solar cycles [9]. GSMF polarity influences the drift of positive and negative particles in the heliosphere at solar minimum [10]. During positive heliomagnetic field polarity, positive charged particles reach the Earth most likely from the polar regions of the heliosphere, while negative charged particles (e^-,$\overline{p}$) come mainly from the ecliptic regions along the heliospheric current sheet (HCS). An opposite situation holds during negative magnetic field polarity epochs. Particle fluxes propagating along the HCS are more modulated with respect to those coming from the poles. The transition from the positive GSMF polarity to negative leads to an increasing modulation coefficient, but the reverse transition leads to a decreasing one on the bulk of positive GCR [11]. The maximum proton and helium flux expected reduction during a negative polarity epoch with respect to a positive one at solar minimum is shown in Fig. 8.

A north-south asymmetry in electron and proton fluxes depending on solar activity and on the interplanetary magnetic field (IMF) sector structure and sign has also been observed.

The high energy particle concentration in the northern and southern heliosphere may be different with the excess value and sign being dependent on particle energy. The IMF sector structure reduces the variations in the value rather than sign of asymmetry. The value of the asymmetry (typically of a few %) in galactic cosmic rays has been found to increase little with energy and the asymmetry sign to revert during solar maximum [12].

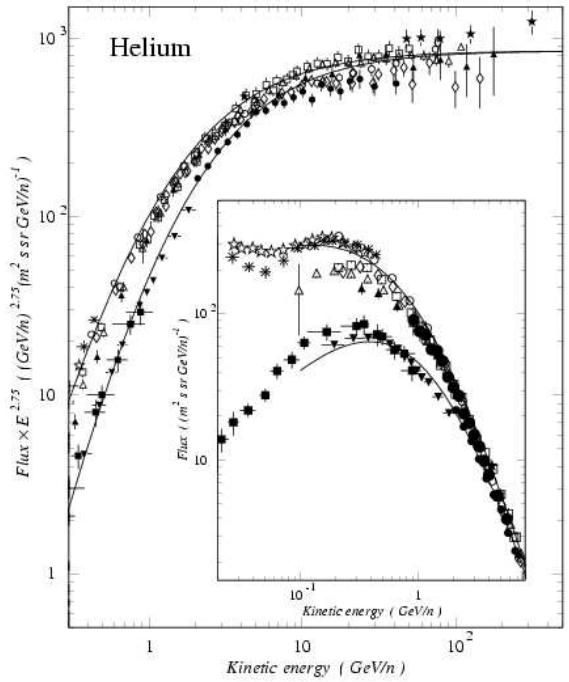

Fig. 7. Same as Fig. 6 for helium nuclei.

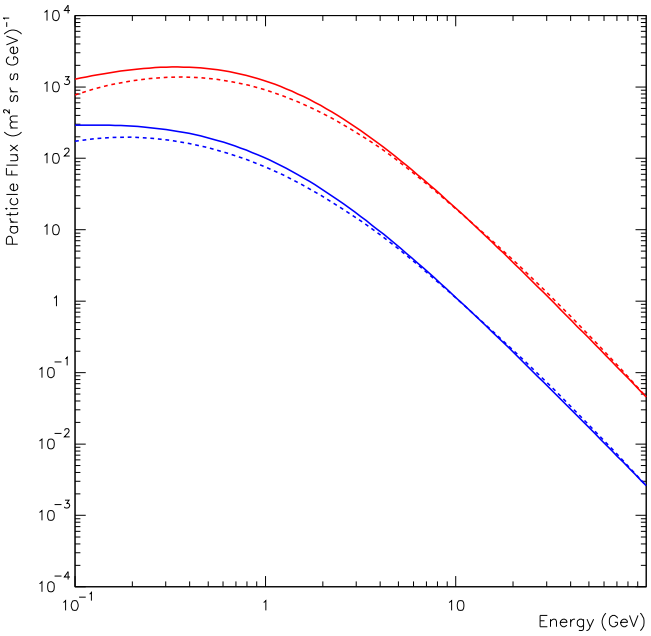

Fig. 8. Maximum expected reduction (dashed lines) of primary p and He nucleus fluxes during a negative polarity epoch with respect to a positive polarity (solid lines) period at solar minimum.

In Figs. 9 and 10 we have reported the interstellar, interplanetary and primary electron flux calculations and measurements carried out in the last 20 years near Earth, during different solar activity and polarity epochs (references to data are reported in [13] and [14]). The calculated electron fluxes at the interstellar medium according to [15]–[17] have been shown as thick dotted and thin continuous lines. The Moskalenko and Strong estimate is of about one order of magnitude larger at 100 MeV while shows a similar trend with respect to Stephens calculations above 1 GeV. The Ferreira et al. [18] computation developed for the Ulysses mission at 120 AU is in better agreement with the Moskalenko and Strong and Protheroe [19] model. The dark region represents the e^- spectrum inferred from radio observations [20]. It is interesting to notice that the Golden et al., 1984 data extrapolated to the interstellar medium agree well with calculations and radio observations. The thick solid and dotted lines in Fig. 9 represent the maximum and minimum contribution, respectively, of jovian electrons [21]. In the same figure the bottom thick dot-dashed line and the thick continuous line in Fig. 10 represent the interplanetary electron fluxes calculated at 1 AU during a quiet and negative (A<0) or positive (A>0) polarity epoch, respectively [18]. It is possible to note that interplanetary electrons overcome of a few orders of magnitude those of primary origin below 1 GeV and that the Ferreira et al. calculation reproduces very well the trend of the Evenson et al. data (large diamonds) in Fig. 9 gathered during a negative solar polarity epoch far from Earth magnetic field. In [18] it is indicated that interplanetary electron fluxes are not majorly affected by solar modulation. A very different situation holds for primary electrons observed at the top of the atmosphere. In Figs. 9 and 10 a modulation parameter ϕ of 400 MV/c (low solar modulation, thin dashed line), 550 MV/c (average solar modulation, thin dot-dashed line) and 1200 MV/c (high solar modulation, thin dotted line) has been considered, respectively, to extrapolate the Stephens calculation near Earth for comparison to the data.

Recently it has been shown that the solar modulation causes up to a factor 2 variation in the LISA test mass charging [1], [7] and that the role of cosmic-ray rare particles cannot be disregarded. In particular, interplanetary electrons and heavy nuclei account for 20% of the total charge deposited in the test masses by galactic protons. Interplanetary electrons play an important role mainly at solar maximum when drastically reduce the absolute charge deposited in the test masses by galactic positive particles but increase the experiment overall shot noise.

Solar polarity change has been found to generate up to 20% variation in the deposited charge [7] and short time GCR flux fluctuations generate coherent signals that cannot be distinguished from genuine gravitational wave transit in LISA [22].

To conclude, in case the proposition to place an electron monitor on board will be accepted, LISA will give us the opportunity to monitor positive and negative GCR within one degree in latitude for up to 10 years.

The role of the GSMF polarity in modulating galactic cosmic-ray fluxes of different charge remains an issue of major importance in the study of cosmic-ray particles such as antiprotons and positrons [23].

V. Solar physics with LISA

The important contribution that LISA will give to solar physics investigations was firstly reported in Grimani and Vocca, 2005 [24].

In the following we highlight the most important characteristics of events that we will be able to observe on LISA for solar physics and space weather investigations.

A. Gradual and impulsive solar events

Energetic protons, heavy nuclei and electrons of solar origin will contribute to the charging of the LISA test masses. Proton and heavy nucleus minimum energy for test-mass charging is 100 MeV(/n). This energy cut-off lowers to a few tens of MeV for the more penetrating electrons.

Impulsive and gradual events are capable to accelerate particles at these energies. Solar particles associated with impulsive and gradual events present different compositions and energy fluxes. In particular, impulsive events are electron rich and do not accelerate electrons above a few tens of MeV and nuclei above 50 MeV/n. Their contribution to the LISA test-mass charging is therefore related to electrons only. In Fig. 11 we have reported the electron fluxes generated by two strong impulsive solar events (September 7th 1973 and November 3rd 1973). The dotted and dot-dashed curves have

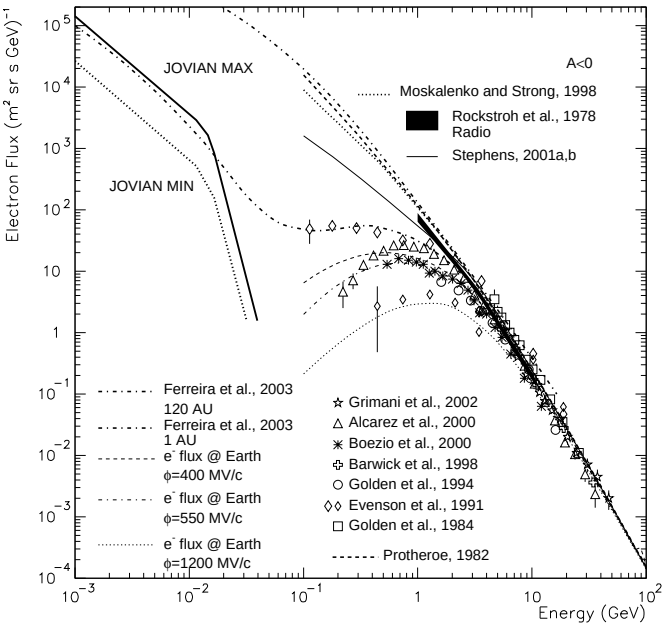

Fig. 9. Interstellar (top thick dot-dashed line [18]; thick dashed line [19]; thick dotted line [15]; continuous line [16], [17]), interplanetary (bottom thick dot-dashed line [18] during a negative polarity epoch) and primary near Earth (dashed line - modulation parameter ϕ=400 MV/c; dot-dashed line ϕ=550 MV/c; dotted line ϕ=1200 MV/c [16], [17]) electron flux calculations. Minimum (thick dotted line) and maximum (thick continuous line) contribution of jovian electron flux is indicated [21]. Symbols represent electron flux measurements at 1 AU.

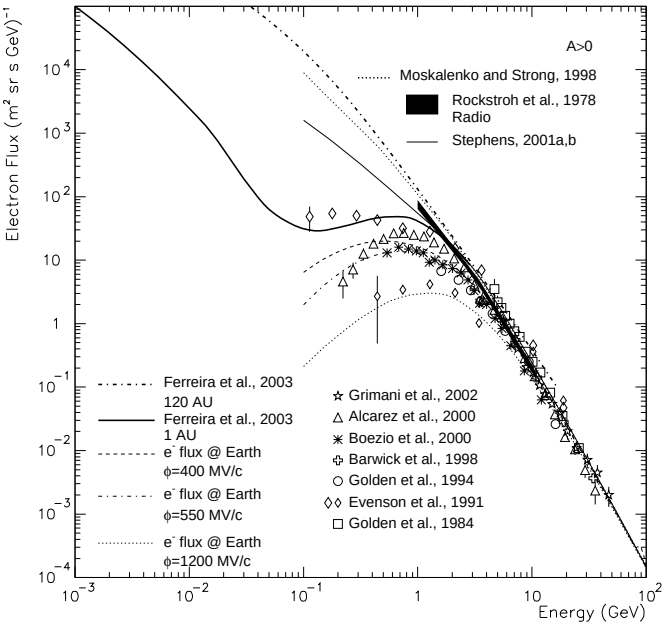

Fig. 10. Interplanetary and primary electron flux measurements and calculations during a positive GSMF polarity epoch. Symbols and curve are defined in Fig. 9.

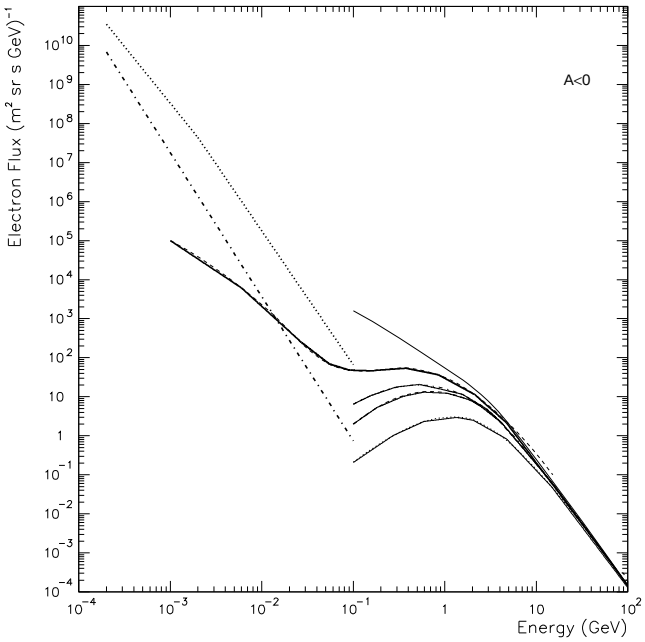

Fig. 11. Solar (thick dotted line - Flare September 7th 1973; thick dot-dashed line - Flare November 3rd 1973), interstellar (thin continuous line) [16], [17], interplanetary during a negative polarity epoch (thick continuous line) [18] and primary electron fluxes (three bottom curves for different solar modulation condition [14].

been artificially extrapolated to 100 MeV in order to compare them to interplanetary (thick continuous line) and to best-fitted electron fluxes observed near Earth. Solar electron fluxes overcome of many orders of magnitude the interplanetary ones below 1 MeV but play a minor role in the LISA test-mass charging being poorly populated above a few MeV. In particular, solar electrons release less than 4% of the total amount of charge deposited in the test masses by GCR.

Solar energetic particles associated with evolving Coronal Mass Ejections are rich of proton and helium particles presenting energies well above tens of GeV. In Figs. 12, 13 and 14 we have reported proton fluxes related to evolving gradual events of different intensity near peak. A comparison with galactic protons at both solar minimum and maximum and with peak fluxes of various fluence events is also shown. It has to be stressed that events pure gradual are rare. Very often impulsive components are present in gradual events. Strong solar events overcome the LISA noise budget [3]. The present radiation monitor design is optimized to map the transit of gradual events. However, it would be of major importance to monitor fast, impulsive components in gradual events as warning of an incoming SEP event as well. We expect an average of a few gradual events per year during the LISA mission [22]. A duration of each event is of a few days. An on board electron monitor will allow us to optimize the test-mass discharging and, consequently, to increase the experiment duty cycle.

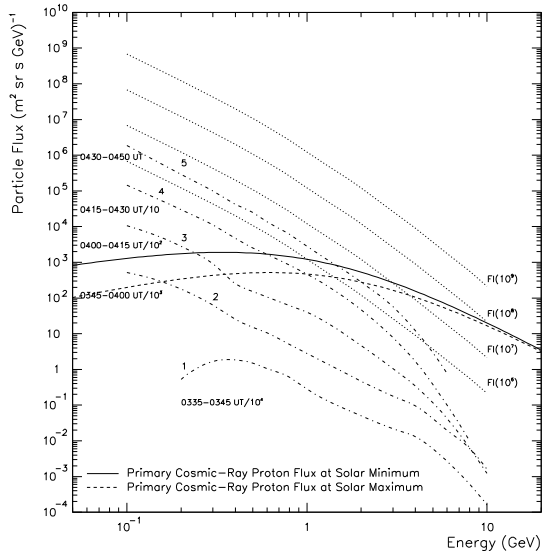

Fig. 12. Solar proton spectra reaching Earth as a function of time during the May 7th 1978 flare (dot-dashed lines). The dotted lines represent various fluence peak fluxes generated by SEPs in units of protons/cm^2. The continuos and dashed lines correspond to primary cosmic-ray proton fluxes at solar minimum and maximum, respectively.

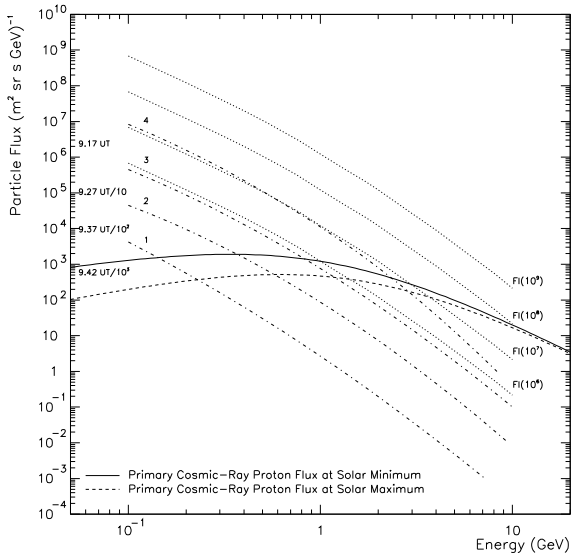

Fig. 13. Solar proton spectra reaching Earth as a function of time during the February 16th 1984 flare (dot-dashed lines). The dotted lines represent various fluence peak fluxes generated by SEPs in units of protons/cm^2. The continuous and dashed lines correspond to primary cosmic-ray proton flux at solar minimum and maximum, respectively.

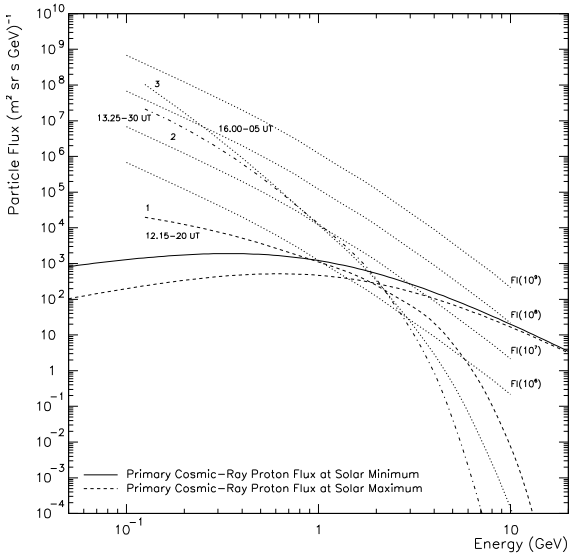

Fig. 14. Solar proton spectra reaching the Earth as a function of time during the September 29th 1989 flare (thick lines). The dotted lines represent various fluence peak fluxes generated by SEPs. The continuous and dashed lines correspond to primary cosmic-ray proton flux at solar minimum and maximum, respectively.

B. Latitude and longitude dependence of solar energetic particle fluxes

SEP fluxes are both latitude and longitude dependent. Dalla et al. [25], for example, have reported a comparison between SEP fluxes measured by Ulysses (63° N and 1.63 AU from the Sun) and SOHO (in the ecliptic at 1 AU). The peak intensity at high latitude is typically smaller than that at the ecliptic and it occurs at a later time. The decay phase is characterized by a similar decay time at the two locations. A study of the longitude dependence of the spatial and temporal distributions of SEPs has been debated [26], [27]. Time profiles of SEPs are affected by the evolution of the intersection point between the observer magnetic field line and the shock. This point sweeps rapidly eastward across the the face of the shock with time at a rate of 27°-45° per day compared to solar rotation of 13° per day. The stronger acceleration occurs near the nose of the shock while the shock strength and the acceleration weaken around either flank. These regions are characterized by the detection of nearly invariant SEP spectra as a function of the longitude. Small shock CMEs are expected to cause rapid changes in intensity. Large CMEs shocks might generate flat longitude profiles in even widely separated spacecraft. Large events can cover up to 90° in longitude.

C. SEP fluxes on the three LISA spacecraft

Shocks of gradual flares generated between 60° E and 120° W are observed to reach Earth [28]. In particular, solar activity observed near 60° W has been associated with particle production in the GeV range observed near Earth [29]. Large CME shocks reaching Earth will go through LISA as well. In

Fig. 15 we have reported the expected countrate variation in each LISA telescope for coincidence particles at the passage of solar proton fluxes reported in Figs. 12, 13 and 14. The indexes in Fig. 15 indicate corresponding fluxes in Figs. 12, 13, 14. As it is possible to notice, at the transit of solar events, the detected radiation monitor countrate will change, for various intensity events, up to four orders of magnitude with respect to incident GCR only. Radiation monitor flux profiles will tell us about the direction of incoming events. The expected countrate for two typical events traversing the radiation monitors from east and from west, respectively, are reported in figures 16 and 17. We have not found in literature a modelization of SEPs at small steps in longitude above 100 MeV(/n). Therefore, we have tried to estimate the SEP flux difference among the LISA spacecraft extrapolating to 2° in longitude SEP fluxes observed at a few degrees in longitude [22]. We have found a possible, reasonable 10% - 15% incident SEP flux difference in the longitude range covered by LISA. We are aware that further work is needed since this is just a rough estimate being related to events characterized by different conditions of the interplanetary magnetic field and solar wind velocity.

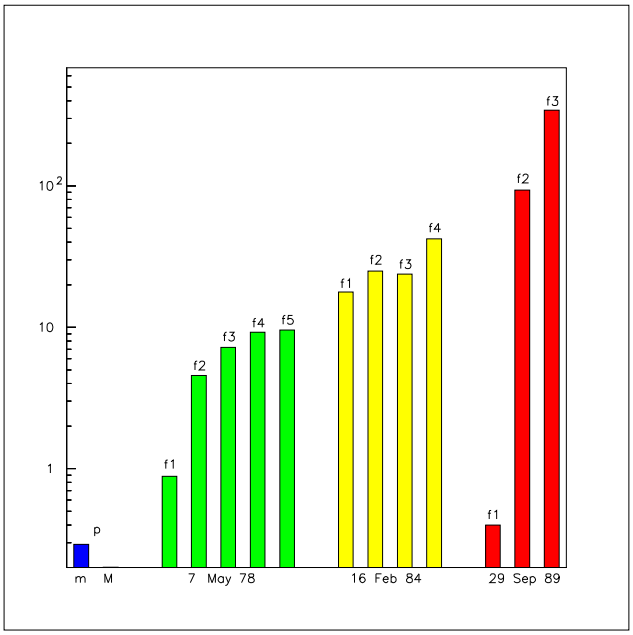

Fig. 15. LISA particle monitor countrate generated by incident galactic protons at solar minimum (m) and solar maximum (M). A comparison is made with the countrate generated by proton fluxes observed near peak of various intensity solar events.

VI. Simulated GCR and SEP observations on LISA radiation monitors

In Figs. 18 and 19 we have reported the simulated [30], [31] ionization energy losses in the radiation monitor silicon wafers for incident galactic proton and helium nucleus fluxes and those generated by SEPs associated with the peak flux of the May 7th 1978 flare. For helium composition in gradual flares, we have considered an uncertainty of one order of magnitude, since p/He ratio is supposed to be about 10 in impulsive flares and about 100 in gradual ones. LISA measurements will allow us to detect impulsive components in gradual flares. It can be noticed that in addition to the expected variation in the countrate at flare transit, the ionization energy losses will appear very different for incident galactic and solar particle fluxes. In particular, ionization energy depositions will allow us to detect small flares.

Mapping fluxes and composition of SEPs is very important for solar physics and space weather investigations. Large gradual flares endanger human life. The level of hazard depends on SEP flux characteristics as a function of energy. The September 29th 1989 flare would have released a dose on astronauts of 4 rem hr^{-1} behind 10 g cm^{-2} of shielding [32]. The dose allowed per year for astronauts is 50 rem and it would be accumulated in half a day to such exposure.

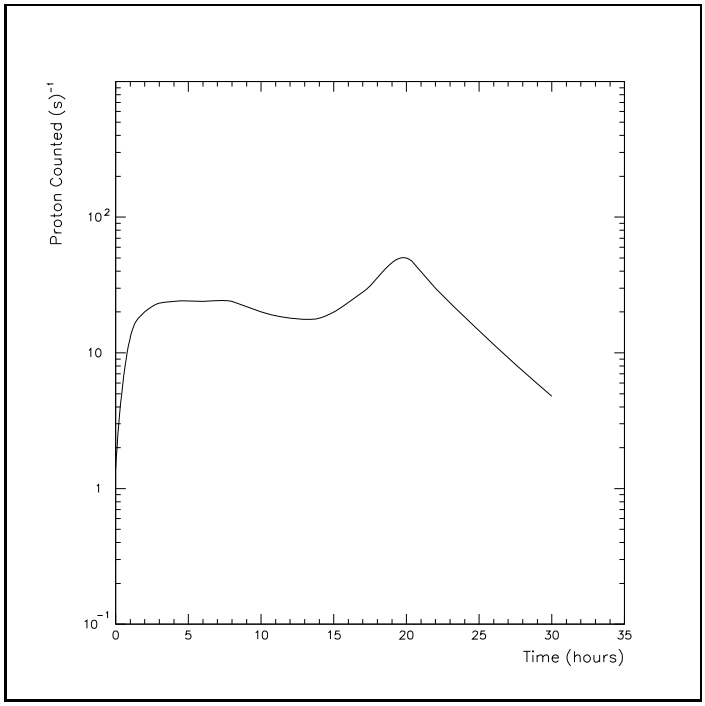

Fig. 16. Expected countrate variation on each LISA radiation monitor for a typical central-eastern event.

VII. Conclusions

We have reported important topics of galactic cosmic-ray and solar physics that the LISA missions will allow us to investigate.

In particular, we will study both long and short-time variations and fluctuations of galactic cosmic rays. Among them, we are particularly interested in studying drift effects for various solar polarity conditions that are of major importance

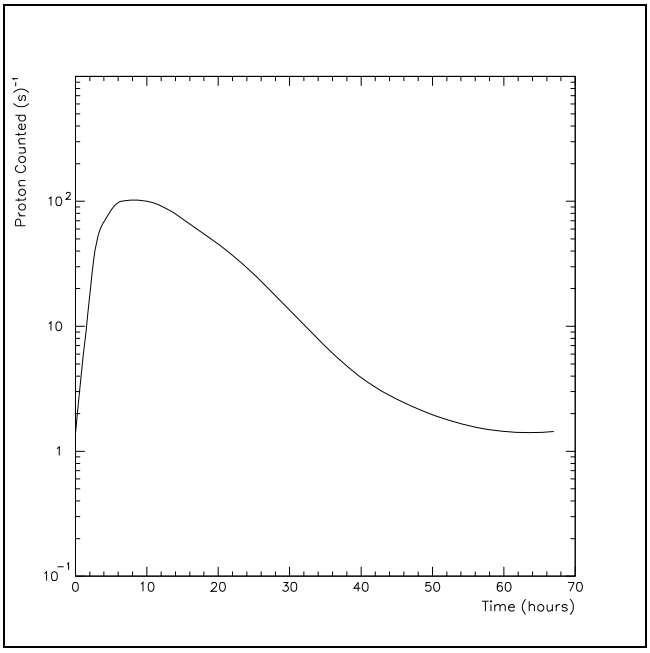

Fig. 17. Expected countrate variation on each LISA radiation monitor for a typical western event.

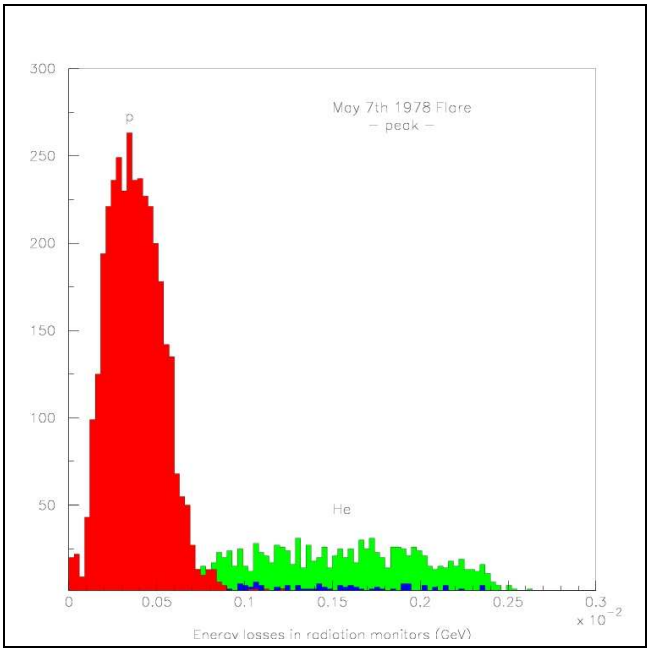

Fig. 19. Simulated ionization energy losses in one silicon wafer for solar particles (peak flux May 7th 1978 flare) traversing the telescope. Clear and dark area for helium nuclei indicate a flare composition of p/He=10 and p/He=100, respectively.

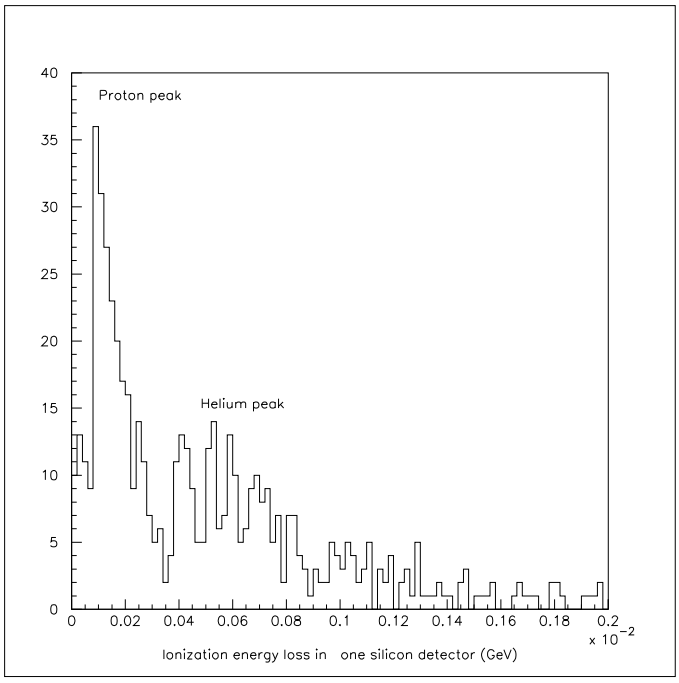

Fig. 18. Simulated ionization energy losses in one silicon wafer for galactic proton and helium nuclei at solar minimum.

to understand correctly rare particle observations in cosmic rays at low energies.

LISA will offer the first possibility to map SEP flux characteristics and composition at small steps in longitude. These studies are of major importance to solar physics and space weather investigations.

REFERENCES

[1] H. M. Araùjo *et al.*, "Detailed calculation of test-mass charging in the LISA mission", *Astr. Phys.*, vol. 22, pp. 451–469, 2005.

[2] C. Grimani *et al.*, "LISA test-mass charging process due to cosmic-ray nuclei and electrons", *CQG*, vol. 22, pp. S327–S332, 2005.

[3] H. Vocca *et al.*, "Simulation of the charging processes of the LISA test masses due to solar particles", *CQG*, vol. 22, pp. S319–S325, 2005.

[4] M. Schulte *et al.*, "Charge management for LISA Pathfinder and development for LISA", to appear on the 6th LISA Symp. Proc.

[5] D. Shaul, H. M. Araùjo, G. Rochester, T. Sumner, and P. Wass, "Evaluation of disturbances due to test mass charging for LISA", *CQG*, vol. 22, pp. S297–S309, 2005.

[6] A. Lobo, "DDS science requirements", 2004, IEEC Internal Note.

[7] C. Grimani *et al.*, "Galactic and interplanetary cosmic rays relevant for LISA test-mass charging", to appear on the 6th LISA Symp. Proc.

[8] ——, "Cosmic-ray spectra near the LISA orbit", *CQG*, vol. 21, pp. S629–S633, 2004.

[9] J. M. Clem and P. A. Evenson, "Observations of cosmic-ray electrons and positrons during the early stages of the A- magnetic polarity epoch", *J. Geophys. Res.*, vol. 109, no. A7, 2004.

[10] G. Boella *et al.*, "Evidence for charge drift modulation at intermediate solar activity from the flux variation of protons and α particles", *J. Geophys. Res.*, vol. 106, pp. 355–362, 2001.

[11] A. V. Belov, R. T. Gushchina, and V. G. Yanke, "Long-term cosmic ray variations: spectrum and relation with solar activity", in *Proc. 25th International Cosmic Ray Conference*, Durban, South Africa, pp. 3911–3914, 1999.

[12] E. V. Gorchakov and Y. V. Mineev, "North-south asymmetry in the electron and proton fluxes dependences on their energy and on solar activity", in *Proc. 27th International Cosmic Ray Conference*, Hamburg, Germany, pp. 3948–3951, 2001.

[13] E. Evenson, P. Tuska and J. Esposito, "Modulation of 1-10 GeV cosmic electrons", in *22nd Int. Cosm. Ray Conf.*, Dublin, Ireland, vol. 3, pp. 505–508, 1991.
[14] C. Grimani *et al.*, "Measurements of the absolute energy spectra of cosmic-ray positrons and electrons above 7 GeV", *A&A*, vol. 392, pp. 287–294, 2002.
[15] I. V. Moskalenko and A. W. Strong, "Production and propagation of cosmic-ray positrons and electrons", *Ap. J.*, vol. 493, pp. 694–707, 1998.
[16] S. A. Stephens, "Plerion as a source of primary cosmic ray electrons", in *27th Int. Cosm. Ray Conf.*, Hamburg, Germany, vol. 5, pp. 1799–1802, 2001.
[17] ——, "Origin of cosmic ray electrons", *Adv. Sp. Res.*, vol. 27, pp. 687–692, 2001.
[18] S. E. S. Ferreira *et al.*, "Solar wind effects on the transport of 3-10 MeV cosmic-ray electrons from solar minimum to solar maximum", *Ap. J.*, vol. 594, pp. 552–560, 2003.
[19] R. J. Protheroe, "On the nature of the cosmic-ray positron spectrum", *Ap. J.*, vol. 254, pp. 391–397, 1982.
[20] J. M. Rockstroh and W. R. Webber, "A new determination of the local interstellar electron spectrum from the radio background", *Ap. J.*, vol. 224, pp. 677–690, 1978.
[21] P. Nieminen, "Spectral input code for induced x-ray emission calculations from solar system bodies", Internal ESTEC working paper, no. 2009, 1999.
[22] D. Shaul *et al.*, "Solar and cosmic ray physics and the space environment studies for and with LISA", to appear on the 6th LISA Symp. Proc.
[23] C. Grimani, "Antimatter origin and average pulsar parameters from e^+ measurements", to appear on 20th European Cosmic Ray Symposium Proc.
[24] C. Grimani and H. Vocca, "Solar physics with LISA", *CQG*, vol. 22, pp. S333–S338, 2005.
[25] S. Dalla *et al.*, "Properties of high heliolatitude solar energetic particle events and constraints on models of acceleration and propagation", *Geophys. Res. Lett.*, vol. 30, no. 19, 8035, 2003.
[26] D. V. Reames, L. M. Barbier, and C. K. Ng, "The spatial distribution of particles accelerated by coronal mass ejection–driven shocks", *Ap. J.*, vol. 466, pp. 473–486, 1996.
[27] D. V. Reames, S. W. Kahler, and C. K. Ng, "Spatial and temporal invariance in the spectra of energetic particles in gradual solar events", *Ap. J.*, vol. 491, pp. 414–420, 1997.
[28] M. A. Shea and D. F. Smart, "Solar proton and GLE event frequency: 1955-2000", in *27th Int. Cosm. Ray Conf.*, Hamburg, Germany, pp. 3401–3404, 2001.
[29] D. F. Smart and M. A. Shea, "The heliolongitudinal distribution of solar flares associated with solar proton events", *Adv. Sp. Res.*, vol. 17, p. 116, 1996.
[30] A. Ferrari, P. R. Sala, A. Fassò, and J. Ranft, "FLUKA: A multi-particle transport code (program version 2005)", CERN-2005-010.
[31] A. Fassò, A. Ferrari, S. Roesler, P. R. Sala, F. Ballarini, A. Ottolenghi, G. Battistoni, F. Cerutti, E. Gadioli, M. V. Garzelli, A. Empl, and J. Ranft, "The physics models of FLUKA: status and recent development", 2003. [Online]. Available: http://www.citebase.org/abstract?id=oai:arXiv.org:hep-ph/0306267
[32] D. V. Reames, "SEPs: Space weather hazard in interplanetary space", Chapman Conference on Space Weather: Progress and Challenges in Research and Applications, Clearwater, FL, March 20-24, 2000.